CASSCF and CAS+1+2 Studies on the Potential Energy Surface and the Rate Constants for the Reactions between CH_2 and O_2

De-Cai Fang* and Xiao-Yuan Fu

Department of Chemistry, Beijing Normal University, Beijing 100875, People's Republic of China

Received: November 9, 2001; In Final Form: January 16, 2002

CAS(14,12)/cc-pvdz calculations are reported for the reaction of $^3CH_2+^3O_2\rightarrow$products. On the singlet potential energy surface, a transition state has been located with an energy barrier of 1.65 kcal/mol, which is in good agreement with the experimental estimation of 1.0−1.5 kcal/mol. The rearrangement and metathesis of the singlet intermediates have been also investigated at the same level of theory. For the triplet case, the formation of CH_2OO has an energy barrier of 5.79 kcal/mol, and the formed triplet CH_2OO could be further decomposed into $CH_2O+O(^3P)$ with an energy barrier of 2.92 kcal/mol. The geometries of some key points have been relocated at the CAS(8,6)+1+2/cc-pvdz level of theory for comparison. The present theoretical results for the total reaction rates, at the CAS(8,6)+1+2/cc-pvdz level, can be expressed by the three-parameter expression: $k(T) = 4.273\times10^{-18}T^{2.245}\exp(-185/T)$ within ±5% error at the temperature range 295−2600 K.

I. Introduction

Triplet methylene($^3CH_2$) is a radical, found in chemical processes such as the combustion of acetylene. Direct measurements of the rate constants for the reactions of $^3CH_2$ with some common species as O_2, NO, and C_2H_2 have been made within the past 20 years.[1−6] As for the titled reaction, a possible reaction mechanism with four intermediates was suggested by Alvarez et al.[7](see Figure 1). Four distinct isomeric species exist as potential minima on the CH_2O_2 hypersurface as shown in Figure 1. Ab initio calculations on the energies and geometries of the low-lying electronic states of the species **I**−**IV** have been reviewed.[8] Moreover, energy barriers to some of the interconversions between species **I**−**IV** and barriers for their decomposition have also been calculated previously.[9−18]

Recently, Su H. et al.[19] have studied the reactions of $^3CH_2$ and $^1CH_2$ with O_2 by time-resolved FTIR spectroscopy, which is mainly focused on the vibrational populations of the reaction products. The branching ratio of the two main products, CO/CO_2 was reported to be 4 by Dombrowsky et al.[6] and near 1 by Alvarez et al.[7] Alvarez et al. also reported 16% yield of H_2CO and indirectly estimated 30% yield of OH.

The rate constant of the reaction of $^3CH_2+^3O_2$ has been measured to be $(3.2 \pm 0.3) \times 10^{-12}$ cm^3 molecule^{-1} s^{-1}. [2−4] A slight temperature dependence of the rate constant was measured over the ranges 233−433[4] and 295−600k,[5] suggesting the presence of a small barrier(1.0−1.5[4] or 1.5 ± 0.3[5] kcal/mol) to the formation of the initial CH_2OO adduct (**I**) or to its subsequent isomerization or fragmentation. Although several theoretical study papers have been published on the interconversions between species **I**−**IV**; however, no theoretical data has been reported for the formation process of CH_2OO(**I**). Therefore, in the present paper, ab initio calculations based on CASSCF wave functions have been performed to explore the potential energy surfaces for the reactions between $^3CH_2$ and $^3O_2$.

* To whom correspondence should be addressed. Email: dcfang@bnu.edu.cn. Fax: 86-10-62200567.

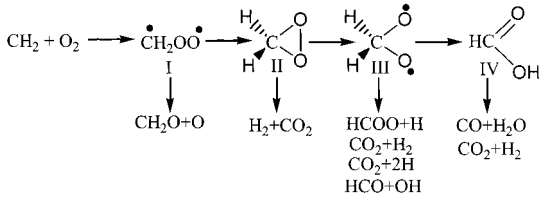

Figure 1. The possible reaction paths suggested by Alvarez et al.[7]

II. Computational Details

All calculations employ the Dunning,[20] cc-pvdz basis set. Two levels of complete active space self-consistent field[21−23] (CASSCF) calculations were done. The larger CASSCF reference wave function is a nearly full valence CAS(except 2s orbitals of O atoms), which consists of 14 active electrons and 12 active orbitals (denoted as CAS(14,12)). The geometric locations and vibrational analysis were mainly using CAS(14,12) method. It was not feasible to perform multireference configuration interaction (MR−CI) calculations using this reference wave function. For the MR−CI calculations, the reference wave function was reduced to a six-orbital, eight-electron active space, denoted as CAS(8,6). The internally contracted MR−CI calculations[24,25] include all single and double excitations relative to the CAS(8,6) reference wave function. These calculations will be denoted as CAS+1+2. For the key points, CAS+1+2 calculations have been employed to locate the geometric parameters for comparison. The CAS and CAS+1+2 calculations were done using the MOLPRO[26] program.

The rate constants were calculated with conventional transition state theory using the POLYRATE 8.2[27] program. The effect of replacing the harmonic oscillator partition function for the out-of-plane mode with a hindered rotation partition function[28,29] was also investigated.

III. Results and Discussions

1. Singlet Surface. On this surface, the extensive search revealed that there are two different approaching modes: (1)

10.1021/jp014129m CCC: $22.00 © 2002 American Chemical Society
Published on Web 02/26/2002

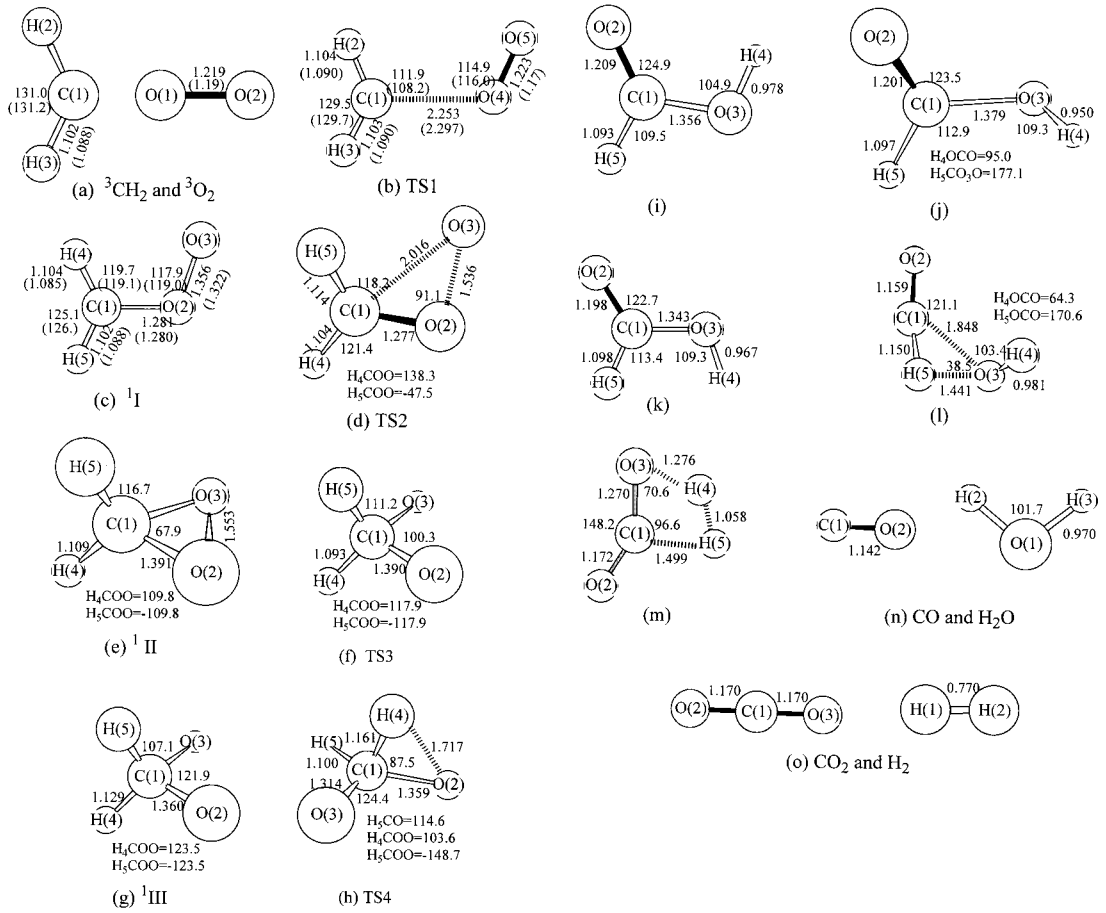

Figure 2. The optimized geometries for the stationary points on the singlet energy surface (the values in parentheses are obtained from CAS-(8,6)+1+2/cc-pvdz calculations).

all atoms on the same plane with Cs symmetry and (2) twisted CH_2 group, but also with C_s symmetry. The geometries of all the possible stationary points obtained on this surface are depicted in Figure 2. Comparing the geometries optimized at different methods, the largest difference (0.04 Å) could be found for the distance of C−O in TS1 and all others are less than 0.02 Å. The differences of angles are less than 4°. Therefore, CAS(14,12)/cc-pvdz is good enough to locate the geometries. The distance of C−O is quite large (2.253 Å) in TS1, but it is 1.281 Å in $^1CH_2OO$(**I**), which indicates that C−O bond in $^1CH_2OO$ exhibits some double-bond character. For twisted case, a stationary point has been found along the reaction path, but vibrational analysis shows that such species is a second saddle point (C−O = 2.082 Å), i.e., there are two imaginary frequencies (−333.6i, −212.8i cm^{-1}). We changed the geometric parameters slightly along the first imaginary mode, a saddle point (C−O = 1.419 Å) has also been found, which corresponds to the transition state of the rotation of CH_2 group. The rotation barrier is quite high because the C−O bond in $^1CH_2OO$ is of some double-bond character. However, if it is shifted slightly along the second imaginary mode, it leads to a true transition state (TS1). Therefore, TS1 is the only true transition state on the singlet potential energy surface. The energy barrier is only 1.67 kcal/mol at CAS(14,12)/cc-pvdz level as listed in Table 1. Our best estimate one with zero-point energy correction is 0.7 kcal/mol at CAS(8,6)+1+2/cc-pvdz level, which is quite close to the experimental estimation(1.0−1.5 kcal/mol).[4,5]

The IRC curve at CAS(14,12)/cc-pvdz level in Figure 3a shows that before TS1 the energy potential curve is very flat, and afterward it becomes very steep after TS1. Figure 4a plots the population changes of the orbitals (11, 12, 13, and 14) along reaction coordinate *s* on singlet energy surface, from which one can realize that when $s < -0.75$, the occupation of orbitals is the main reason keeping the curve flat. However near peroxymethylene ($s \approx 1.6$), the occupation of numbers 11 and 12 are close to 2.0 and those of numbers 13 and 14 are approaching 0.0, which means singlet peroxymethylene is in fact not a diradical, but some sort of zwitterions. In our MP2/cc-pvdz calculations both geometries have been obtained, the diradical one has higher energy than that of zwitterion. On the other hand, only a zwitterion one was located at CAS(14,12)/cc-pvdz level of theory. From Figure 4b, one can see that triplet peroxymethylene is a true diradical.

Two-dimensional plot of the potential surface near the TS1 at CAS(14,12)/cc-pvdz level of theory is shown in Figure 5, from which one can realize that there is a maximum near C−O = 2.25 Å and another at O−O = 1.22 Å, and a minimum is located near C−O = 1.3 Å and another at O−O = 1.35 Å. In fact, the global optimization leads to a true minimum at C−O = 1.28 and O−O = 1.36 Å. When C−O bond is kept near 1.3 Å and O−O bond is increased, the curve shows that the energy is always increased, which indicates that this minimum $^1CH_2OO$ is not related to $CH_2O+O(^3P)$ but $CH_2O+O(^1D)$ since the energy of the first one is lower than $^1CH_2OO$. Actually, this minimum can also lead to a three-membered ring intermediate CH_2OO(**II**) via a transition state TS2 (see Figure 2). The energy barrier for this process is 19.7 kcal/mol at CAS(14,12)/cc-pvdz level(close to 21.5 kcal/mol in ref 11). Intermediate CH_2OO-(**III**) seems less stable than CH_2OO(**II**) as shown in Table 2,

TABLE 1: Total Energies (au) and the Relative Energies (kcal/mol)[a]

	CAS(14,12)	CAS+1+2 OPT[a]
$^3CH_2+^3O_2$	−188.669414	−188.974803
	(0.0)	(0.0)
TS1	−188.666790	−188.974634
	(1.64)	(0.11)
$^1CH_2OO(^1\mathbf{I})$	−188.756231	−188.073362
	(−54.38)	(−60.85)
TS2	−188.724873	
	(−34.80)	
$^1CH_2OO(\mathbf{II})$	−188.798993	
	(−81.31)	
TS3	−188.765728	
	(−60.50)	
$^1CH_2OO(\mathbf{III})$	−188.781949	
	(−70.62)	
TS4	−188.778748	
	(−68.61)	
$^1CH_2OO(\mathbf{IV})$	−188.953631	
trans	(−178.35)	
TS5	−188.927954	
	(−162.24)	
$^1CH_2OO(\mathbf{IV})$	−188.944812	
cis	(−172.81)	
TS6	−188.836950	
	(−105.13)	
$CO+H_2O$	−188.956243	
	(−179.99)	
TS7	−188.834879	
	(−103.83)	
CO_2+H_2	−188.971955	
	(−189.85)	
TS8	−188.660189	−188.969347
	(5.79)	(3.42)
$^3CH_2OO(^3\mathbf{I})$	−188.715355	−189.029157
	(−28.83)	(−34.11)
TS9	−188.710702	
	(−25.91)	
$H_2CO+O(^3P)$	−188.794576	
	(−78.54)	

[a] The geometries were optimized at CAS(8,6)+1+2/cc-pvdz level.

and a transition state TS3 could be found between them with energy barrier of 20.8 kcal/mol from **II** to **III**.

The reaction of intermediate **III** might proceed in several ways directly. Keeping the C_{2v} symmetry, we did locate a stationary point for the formation of H_2 and CO_2, but the vibrational analysis showed that this stationary point has two imaginary frequencies (−1272i, −597i cm^{-1}). To eliminate the second imaginary mode, another true transition state TS4 has been located, which corresponds to that for the rearrangement from intermediate **III** to trans-**IV**. Another possible metathesis process is forming H and HC(O)O, however, no transition state could be found between them. In fact, if HC(O)O were involved, the reaction would proceed to CO_2 more easily than to CO,[30,31] which is inconsistent with the branching ratio of CO to CO_2.[6] Therefore, the possible reaction path is the rearrangement from **III** to **IV**. One transition state TS4 has been located along the reaction path, which is only 2 kcal/mol higher than the intermediate **III**. The potential energy surfaces for the reactions from HCOOH to $CO+H_2O$ or to CO_2+H_2 have been reported in some literatures.[17,18] For comparison our CAS(14,12)/cc-pvdz results are also given. The schematic description of the potential energy surfaces for this reaction is shown in Figure 6, from which one can realize that the reaction to CO or CO_2 are all exothermic. The calculated heats of reactions $CH_2+O_2\rightarrow CO+H_2O$ and $CH_2+O_2\rightarrow CO_2+H_2$ are −176.4 and −188.9 kcal/mol at CAS(14,12)/cc-pvdz level (with ZPE correction), respectively, which are quite close to the experimental values.[7,32] The activation energies for the formation of $CO+H_2O$ and CO_2+H_2 from trans-**IV** are 67.9 and 71.3 kcal/mol, respectively, which is almost the same as the results from Goddard et al.[17].

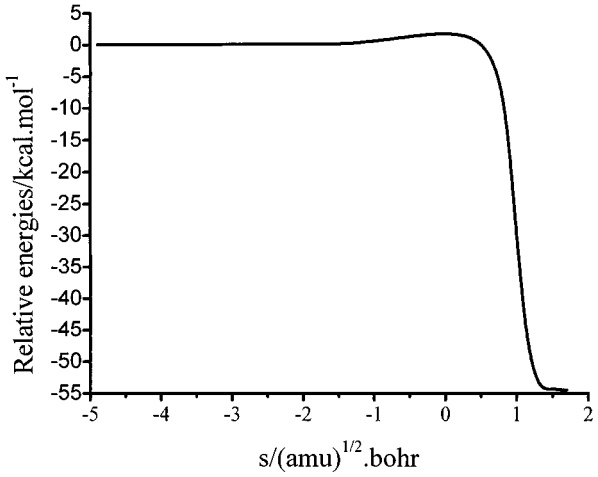

(a) singlet

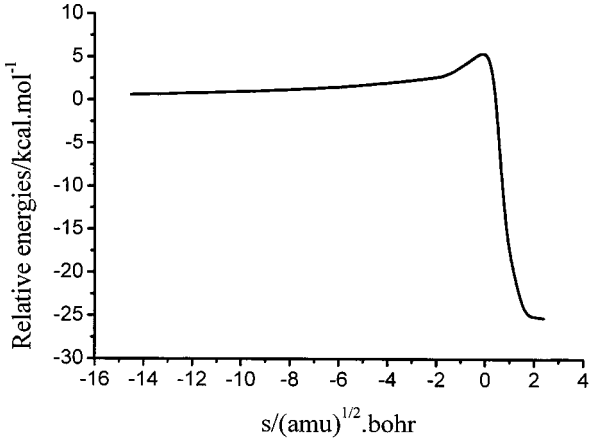

(b) triplet

Figure 3. (a) The energy change along *s* (the reaction coordinate) for $^3CH_2+^3O_2\rightarrow$**I** on the singlet surface. (b) The energy change along *s* on the triplet surface.

2. Triplet Surface. On the triplet surface, we tried to locate all the possible stationary points. Vibrational analysis shows that the true transition state and minimum are with twisted CH_2 as shown in Figure 7. The activation barrier is 5.8 kcal/mol-(see Table 1), about 2 times more than that for the singlet surface. MRCI calculation gives about 3.4 kcal/mol of energy barrier. IRC calculation shows that apart from TS8, one direction could lead to reactants, and another direction leads to the twisted $^3CH_2OO$ (see Figure 3b).

Two-dimensional plot of the potential surface near the TS8 at CAS(14,12)/cc-pvdz level is shown in Figure 8. One can realize that there is a maximum near C−O=2.1 and another O−O=1.22 Å and a minimum near C−O = 1.39 and another O−O = 1.42 Å, which is very close to the optimized one (C−O = 1.38 and C−O = 1.42 Å). Another maximum is near C−O = 1.39 and O−O = 1.60 Å, and the optimized one is at C−O = 1.35 and O−O = 1.51 Å. The metathesis of the triplet CH_2-$OO(^3\mathbf{I})$ could take place via a transition state TS9 with an activation energy of 1.44 kcal/mol (with zero-point energy correction), which is easier to proceed.

TABLE 2: Harmonic Vibrational Frequencies (cm^{-1}) for All the Possible Stationary Points at CAS(14,12)/cc-pvdz Level[a]

	ω_1	ω_2	ω_3	ω_4	ω_5	ω_6	ω_7	ω_8	ω_9
$^3CH_2$	3260	3050	1123						
	(3446)	(3220)	(1192)						
$^3O_2$	1534								
	(1688)								
TS1	3237	3033	1478	1140	384	198	152	141	-234i
	(3430)	(3209)	(1657)	(1196)	(314)	(262)	(122)	(90)	(−162i)
^{1}**I**	3215	3065	1465	1269	1233	849	793	618	537
	(3434)	(3258)	(1513)	(1319)	(1253)	(955)	(741)	(612)	(548)
TS2	3143	2929	1530	1347	1194	951	721	542	-770i
^{1}**II**	3249	2895	1572	1305	1288	1222	1021	923	694
TS3	3189	3130	1568	1440	1117	1083	1063	947	-1764i
^{1}**III**	2873	2814	1274	1192	1120	912	739	575	516
TS4	3100	2625	1319	1296	1134	1011	628	624	-923i
^{1}**IV** trans	3667	3265	1850	1478	1359	1152	1105	683	642
TS5	4132	3215	1861	1479	1288	1121	966	684	-602i
^{1}**IV** cis	3772	3167	1886	1496	1335	1121	1084	663	519
TS6	3665	2717	1918	1120	795	687	365	314	-1764i
CO	2169								
H_2O	3851	3735	1709						
TS7	3756	3214	1767	1297	1142	845	720	608	-2465i
CO_2	2425	1339	654	654					
H_2	4246								
TS8	3227	3026	1384	1149	515	320	218	88	-374i
	(3424)	(3205)	(1578)	(1197)	(467)	(294)	(186)	(82)	(−318i)
^{3}**I**	3362	3121	1461	1186	1057	928	787	488	195
	(3482)	(3308)	(1523)	(1225)	(1072)	(932)	(780)	(475)	(191)
TS9	3361	3043	1500	1190	1104	694	426	226	-745i
H_2CO	2806	2522	1814	1557	1291	1201			

[a] The values in parentheses are obtained by CAS+1+2/cc-pvdz method.

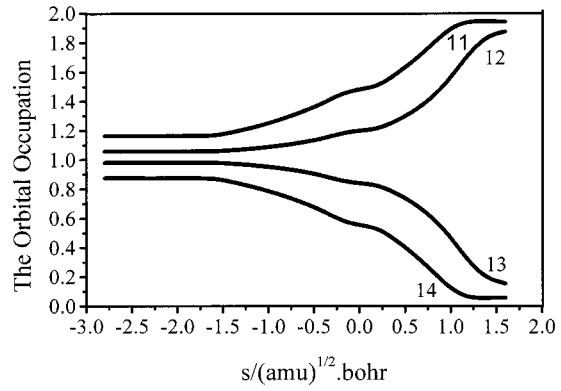

(a)Singlet surface

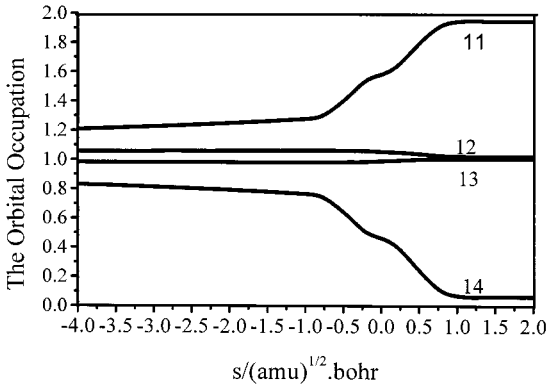

(b) triplet surface

Figure 4. The population changes of the orbitals along *s*: (a) singlet surface and (b) triplet surface.

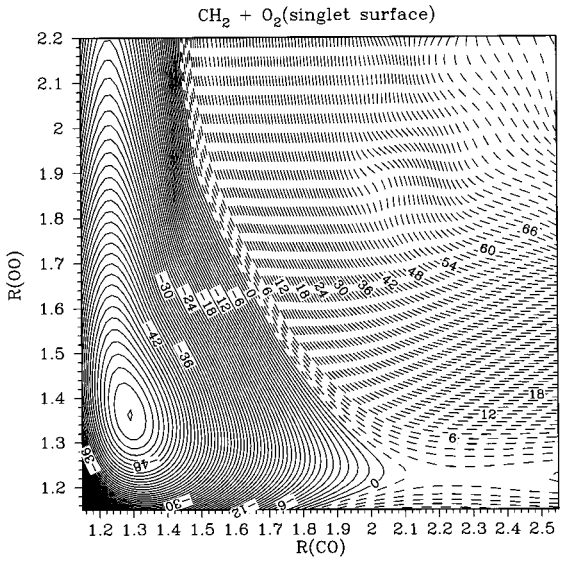

Figure 5. Contour plot of CAS(14,12)/cc-pvdz energies in the vicinity of TS1 on the singlet energy surface for the reaction of $^3CH_2+^3O_2 \rightarrow ^1$**I**. The contour increment is 1.0 kcal/mol. The solid contours denote energies below $^3O_2+^3CH_2$; dashed contours denote energies above $^3O_2+^3CH_2$.

3. The Rate Constants for the Reaction $^3O_2+^3CH_2 \rightarrow$ Products. To get more accurate rate constants, CAS+1+2/cc-pvdz has been employed to locate the some key species, such as CH_2, O_2, TS1, TS8, and intermediates ^{1}**I** and ^{3}**I**. The vibrational analysis was done at the same level. The geometries, energies, and vibrational frequencies obtained at CAS(8,6)+1+2/cc-pvdz level were used throughout this section.

Figure 9 shows the calculated rate constants, along with the recent experimental values. The calculated ones are in good

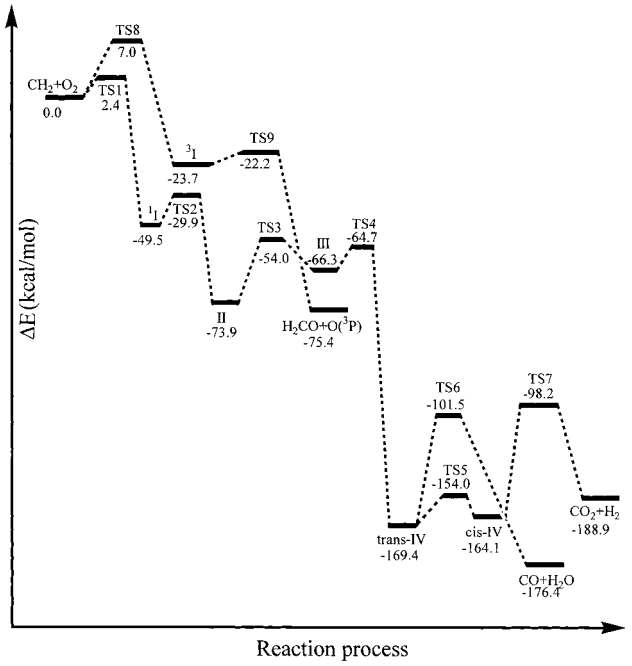

Figure 6. The schematic expression of the possible reaction path for the reaction $CH_2+O_2 \rightarrow$ products (with ZPE correction).

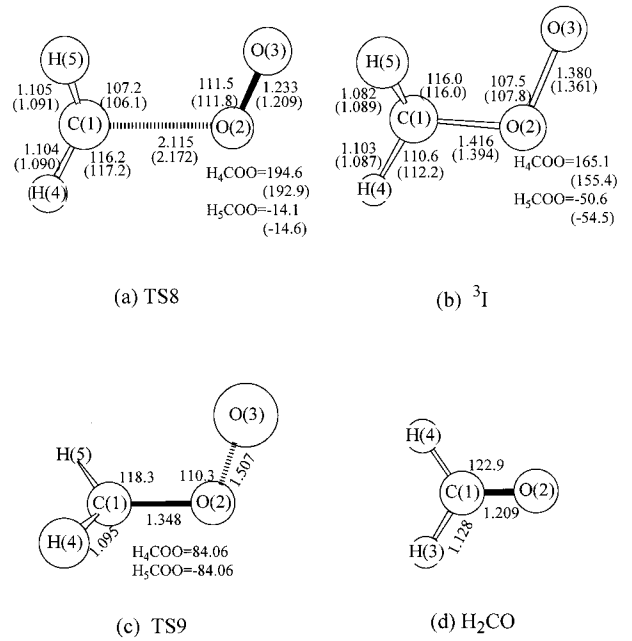

Figure 7. The optimized geometries for the stationary points on the triplet energy surface(the values in parentheses are obtained by CAS-(8,6)+1+2/cc-pvdz calculations).

agreement with the experimental values. To test the hindered rotor contribution to the rate constants, a rotation barrier of 0.99 kcal/mol was calculated by changing the torsion angle HCOO from 0° to 180° for the TS1 geometry, which was located at torsion angle HCOO = 90°. The hindered rotor rate constants are closer to the experimental ones. At higher temperatures (1000−1800 K), a negative temperature dependence has been observed,[6] which is inconsistent with those at lower temperatures. It should be kept in mind, however, that those rate constants at higher temperatures are not determined directly. Our calculations confirm that there is indeed a small barrier between the reactants $^3CH_2+^3O_2$ and intermediates ^{1}**I** or ^{3}**I**. Therefore, our results are closer to the lower temperature case.

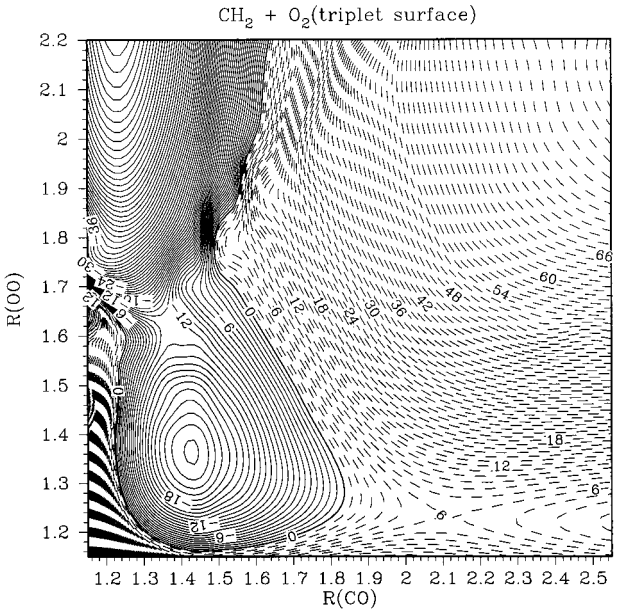

Figure 8. Contour plot of CAS(14,12)/cc-pvdz energies in the vicinity of TS2 on the triplet energy surface for the reaction of $^3CH_2+^3O_2 \rightarrow ^3$**I**. Plotting conventions are the same as in Figure 5.

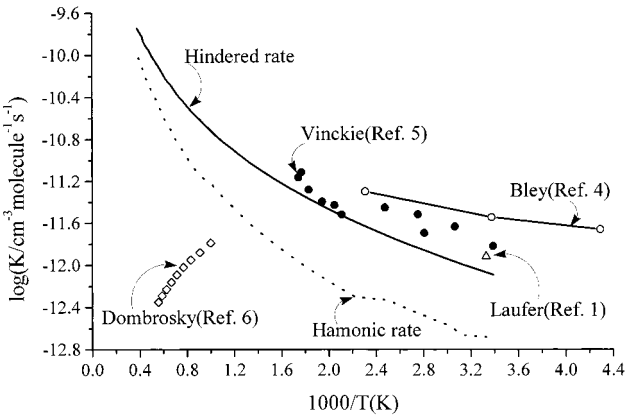

Figure 9. The comparison of the Arrhenius plots of the calculated hindered rotor (solid line) and harmonic(dot line) rate constants vs 1000/*T* to the available experimental data for the titled reaction.

With the data obtained from hindered rotor rate constants, we can fit the rate constant expression to the following equation:

$$k(T) = 4.273 \times 10^{-18} T^{2.245} \exp(-185/T).$$

Acknowledgment. This work was supported by National Natural Science Foundation of China (Grant No. 20073006). The authors also thank Prof. L. B. Harding for providing the contour plotting program and Prof. T. -H. Tang for language polishing.

References and Notes

(1) Laufer, A. H. *Rev. Chem. Intermed.* **1981**, *4*, 225 and references therein.

(2) Darwin, D. C.; Young, A. T., Johnston, H. S.; Moore, C. B. *J. Phys. Chem.* **1989**, *93*, 1074.

(3) Böhland, T.; Temps, F.; Wagner, H. Gg. *Ber. Bunsen-Ges. Phys. Chem.* **1984**, *88*, 455.

(4) Bley, U.; Temps, F.; Wagner, H. Gg.; Wolf, M. *Ber. Bunsen-Ges. Phys. Chem.* **1992**, *96*, 1043.

(5) Vinckier, C.; Debruyn, W. *J. Phys. Chem.* **1979**, *83*, 2057.

(6) Dombrowsky, Ch.; Wagner, H. Gg. *Ber. Bunsen-Ges. Phys. Chem.* **1992**, *96*, 1048.

(7) Alvarez, R. A.; Moore, C. B. *J. Phys. Chem.* **1994**, *98*, 174.

(8) Kafafi, S. A.; Martinez, R. I.; Herron, J. T. In *Modern Models of Bonding and Delocalization*; Leibman, J. F., Greenberg, A., Eds.; VCH: New York, 1988; p 283.
(9) Ha, T.-K.; Kühne, H.; Vaccane, H.; Günthard, Hs. H. *Chem. Phys. Lett.* **1974**, *24*, 172.
(10) Harding, L. B.; Goddard, W. A. *J. Am. Chem. Soc.* **1978**, *100*, 7180.
(11) Karlstrôm, G.; Emgstrôm, S.; Jônsson, B. *Chem. Phys. Lett.* **1979**, *67*, 343.
(12) Cremer, D.; Schmidt, T.; Gauss, J.; Radhakrishnan, T. P. *Angew. Chem., Int. Ed. Engl.* **1988**, *27*, 427.
(13) Bach, R. D.; Andrés, J. L.; Owensby, A. L.; Schlegel, H. B.; McDouall, J. J. W. *J. Am. Chem. Soc.* **1992**, *114*, 7207.
(14) Karlstrôm, G.; Roos, B. O. *Chem. Phys. Lett.* **1981**, *79*, 416.
(15) Cimiraqglia, R.; Ha, T.-K.; Günthard, Hs. H. *Chem. Phys. Lett.* **1982**, *85*, 262.
(16) Dupuis, M.; Lester, W. A. *J. Chem. Phys.* **1984**, *80*, 4193.
(17) Goddard, J. D.; Yamaguchi, Y.; Schaefer, H. F. *J. Chem. Phys.* **1992**, *96*, 1158.
(18) Francisco, J. S. *J. Chem. Phys.* **1992**, *96*, 1167.
(19) Su, H.; Mao, W.; Kong F. *Chem. Phys. Lett.* **2000**, 322, 21.
(20) Woon, D. E.; Dunning, T. H., Jr. *J. Phys. Chem.* **1993**, *98*, 1358.
(21) Roos, B. O.; Taylor, P. R.; Siegbahn, P. E. M. *Chem. Phys.* **1980**, *48*, 157.
(22) Werner H. J.; Knowles, P. J. *J. Chem. Phys.* **1985**, *82*, 5053.
(23) Knowles, P. J.; Werner, H. J. *Chem. Phys. Lett.* **1985**, *115*, 259.
(24) Werner H. J.; Knowles, P. J. *J. Chem. Phys.* **1988**, *89*, 5803.
(25) Knowles, P. J.; Werner, H. J. *Chem. Phys. Lett.* **1988**, *145*, 514
(26) MOLPRO is a package of ab initio programs written by Werner, H.-J., and Knowles, P. J., with contributions from Almlof, J.; Amos, R. D.; Berning, A.; Cooper, D. L.; Deegan, M. J. O.; Dobbyn, A. J.; Eckert, F.; Elbert, S. T.; Hampel, C.; Lindh, R.; Lloyd, A. W.; Meyer, W. Nicklass, A.; Peterson, K.; Pitzer, R.; Stone, A. J.; Taylor, P. R.; Mura, M. E.; Pulay, P.; Schutz, M.; Stoll, H.; Thorsteinsson, T.
(27) Chuang, Y. Y.; Corchado, J. C.; Fast, P. L.; Villa, J.; Hu, W. P.; Liu, Y. P.; Lynch, G. C.; Jackels, C. F.; Nguyen, K. A.; Gu, M..Z.; Rossi, I.; Coitino, E. L.; Clayton, S.; Melissas, V. S.; Steckler, R.; Garret, B. C.; Isaacson, A. D.; Truhlar, D. G. *POLYRATE*, version 8.2; University of Minnesota: Minneapolis, 1999.
(28) Pitzer, K. S. *J. Chem. Phys.* **1946**, *14*, 239.
(29) Chuang, Y. Y.; Truhlar, D. G. *J. Chem. Phys.* **2000**, 112, 1221.
(30) Schatz, G. C.; Fitzcharles, M. S.; Harding, L. B. *Faraday Discuss., Chem. Soc.* **1987**, *74*, 359.
(31) Aoyagi, M.; Kato, S. *J. Chem. Phys.* **1988**, *88*, 6409.
(32) Baulch, D.L.; Cox, R. A.; Hampson, R. F.; Kerr, J. A.; Troe, J.; Watson, R.T. *J. Phys. Chem. Ref. Data*, **1980**, *9*, 295.